ChemComm

Accepted Manuscript

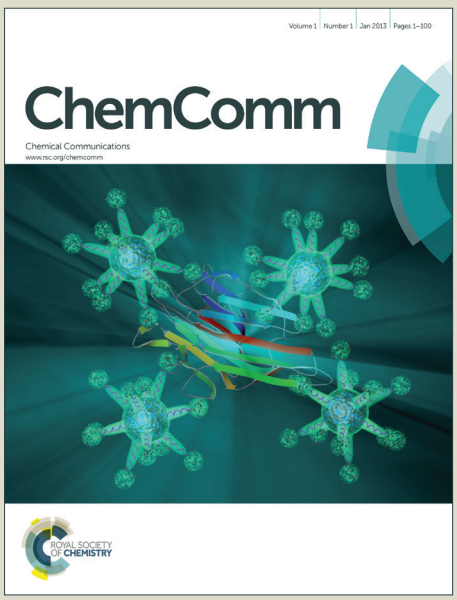

ROYAL SOCIETY OF CHEMISTRY

www.rsc.org/chemcomm

Cite this: DOI: 10.1039/c0xx00000x

www.rsc.org/xxxxxx

COMMUNICATION

Transfer and Control of Molecular Chirality in the 1:2 Host-Guest Supramolecular Complex Consisting of Mg(II) bisporphyrin and Chiral Diols: Effect of H-bonding on Rationalization of Chirality

Sk Asif Ikbal, Sanfaori Brahma, and Sankar Prasad Rath*

Received (in XXX, XXX) Xth XXXXXXXXX 20XX, Accepted Xth XXXXXXXXX 20XX
DOI: 10.1039/b000000x

A clear rationalization of the origin of chirality transfer from an optically active diol guest to an achiral Mg(II)bisporphyrin host in a series of 1:2 host-guest supramolecular complex has been reported here that has so far remained the most outstanding issue for the chirogenic process.

Determination of absolute configuration remains a very important topic in the chemical and biological world.[1] Porphyrins are considered as one of the most useful chromophores for probing molecular chirality of the chiral guests because of its unique property of absorption spectroscopy featuring intense Soret band at the visible region, which is an important prerequisite for efficient chirogenic performance.[1-8] Upon formation of a chiral host–guest supramolecular complex between an achiral bis-metalloporphyrin derivative and a chiral guest, a bisignate CD curve (so-called exciton couplet) is observed in the porphyrin spectral region, which is diagnostic of the guest's absolute configuration.[1]

Stoichiometry controlled supramolecular chirality induction with bifunctional ligands are known to occur via stepwise 1:1 and 1:2 host-guest complexation mechanism. There are also crystallographic reports of chiral 1:1 *sandwich* complex consisting of Zn(II)bisporphyrin host and chiral diamines as guest.[2a,3b-c] However, there are still very limited reports of chirality induction of metallobisporphyrin with chiral alcohols.[2b,5b,c] In the present work, we investigate the effect of stoichiometry on the chirality induction process in the supramolecular complex consisting of Mg(II)bisporphyrin host and chiral vicinal diol as guest. For the first time, a clear rationalization of the chirality induction process has been demonstrated for the 1:2 host-guest complexes with the help of single crystal X-ray structure analysis of one such complex. The chiroptical response of the complexes has been observed to be a direct consequence of the guest chirality, which translates into the helicity of the interacting chromophores.

Free base dibenzothiophene bridged bisporphyrin has been synthesized using a reported procedure[9] and magnesium was inserted into it by adding $MgBr_2.OEt_2$ in dry dichloromethane which after chromatographic purification yielded Mg(II)bisporphyrin, **1**. Upon the addition of chiral diol (2*R*, 3*R*)-2,3-butanediol (L^1) to **1**, two stepwise spectral changes at the UV-visible regions were observed (Fig. S1) depending on the concentration of the guest ligand which are attributed to the formation of 1:1 *sandwich* complex **1**•L^1 and 1:2 host-guest complex **1**•$(L^1)_2$ at low and high substrate concentration regions, respectively.[3a,10] The formation of 1:1 *sandwich* complex is anticipated by gradual decrement accompanied by blue shift of Soret (from 407 to 406 nm) and Q band (from 547 to 546 nm) and the molecule has been isolated in solid and thoroughly characterized. Upon further addition of the guest ligand, Soret band retraced to 407 nm with small increment of intensity but no significant change in Q bands due to the conversion of 1:1 *sandwich* to 1:2 host-guest complex. As the two porphyrin rings are pushed further in 1:2 host-guest complex compared to 1:1 sandwich complex, there occurs a decrement in the interchromophore interaction resulting red shift of the Soret band.

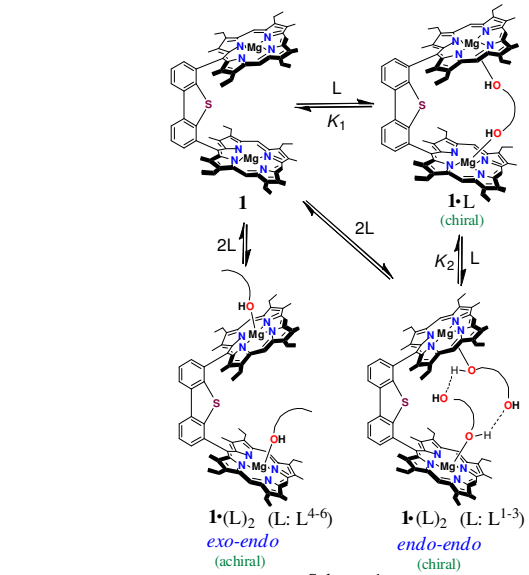

Scheme 1

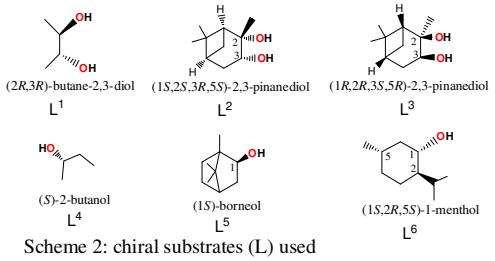

Scheme 2: chiral substrates (L) used

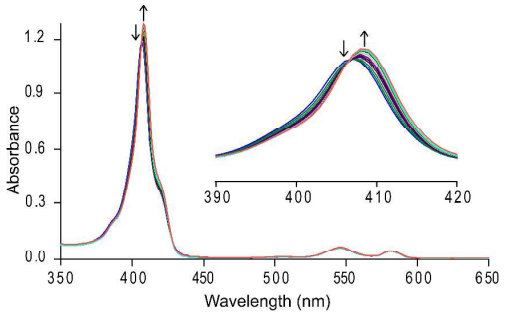

Fig. 1 UV-visible (in CH_2Cl_2 at 295 K) spectral change of **1** (at 3×10^{-6} M) upon addition of L^2 as the host-guest molar ratio change from 1:0 to 1:375. Inset shows the expanded Soret band region.

Similar addition of (1*S*, 2*S*, 3*R*, 5*S*)-2,3-pinanediol (L^2) to **1**, results only the red shift of Soret (from 407 to 409 nm), shoulder (from 421 to 422 nm) and Q band (from 547 to 548 nm) along with an increase in the Soret band intensity (Fig. 1) due to the formation of 1:2 host-guest complex **1**•$(L^2)_2$ which has been isolated and structurally characterized (*vide infra*). Unlike L^1, L^2, however, contains one tertiary carbon attached to one of the –OH group which makes 1:1 *sandwich* complex unstable but suitable for 1:2 *endo-endo* complexation through the less sterically crowded –OH group. Upon addition of (1*R*, 2*R*, 3*S*, 5*R*)-2,3-pinanediol (L^3) to the dichloromethane solution of **1**, similar change in the UV-visible spectrum is obtained. Chiral monoalcohols with similar structure such as (*S*)-2-butanol (L^4), (1*S*)-borneol (L^5) and (1*S*, 2*R*, 5*S*)-1-menthol (L^6) also bind with **1** to give 1:2 host-guest complexes only (Figs. S2-S4); red shifting of Soret band (from 407 to 408 nm) and shoulder (from 421 to 422 nm) are indicative of the 1:2 complexation. Scheme 1 displays all the complexes reported here and their abbreviations while Scheme 2 shows the list of chiral substrates used.

The host-guest stoichiometry of the complexes in solution are determined by Job's continuous variation plot using both UV-vis as well as CD (*vide infra*) spectral change at guest's low concentration regions. It has been found that maximum change in UV-visible and CD amplitude is observed for the binding of **1** with L^1 in dichloromethane at their equimolar concentration (*i.e.*, 0.5 mol fractions) (Fig. S5) indicating the formation of a 1:1 complex. ESI mass spectroscopy reveals peak at m/z 1270.6175 and 1362.7146 which are assigned for [**1**•L^1]+ and [**1**•$(L^1)_2$+2H]+ (Figs. S6 and S7), respectively, confirming the formation of 1:1 *sandwich* and 1:2 host-guest complexes with L^1. However, optimum formation of complex between **1** and L^2 was found at 0.33 mole fraction of host **1** indicating 1:2 host-guest complexation (Fig. S8) which is also structurally characterized (*vide infra*).

Dark red crystals[11] of **1**•$(L^2)_2$ are grown *via* slow diffusion of acetonitrile into dichloromethane solution of the complex at room temperature in air. The complex crystallizes in orthorhombic crystal system with $P2_12_12_1$ chiral space group, a perspective view is depicted in Fig. 2 while the molecular packing is shown in Fig. S9. From the crystal structure, it can be seen that L^2 coordinates to the magnesium centre through –OH(3) binding site in an *endo-endo* fashion. The two Mg(II) centres thus adopt five-coordinate square pyramidal geometry while the metals have been displaced by 0.44 and 0.36 Å from the least-square plane of $C_{20}N_4$ porphyrinato cores. As a consequence of ligand coordination, a lot of conformational changes in the framework of **1**•$(L^2)_2$ occurs. The induction of asymmetry information of the enantiopure chiral ligand to the achiral host is highly anticipated from the unidirectional screw observed in the bisporphyrin moiety. The projection of the binding site at the chiral center (*R*) of L^2 compels two porphyrin rings to be twisted in an anticlockwise direction around the rigid dibenzothiophene bridge with a torsion angle Φ (Mg1-C33-C43-Mg2) of -3.80° in order to minimize the host–guest steric interactions. It has also been observed that two diol ligands lying inside the bisporphyrin cavity are prevented from free movements due to two strong inter-ligand H-bonding between the OH groups (O1•••O4, 2.747(3); O2•••O4, 2.938(3) and O2•••O3, 2.842(3) Å) which eventually interlock two porphyrin rings stereospecifically. Thus, the crystallographic data clearly rationalize the origin of the optical activity in the supramolecular 1:2 host-guest complex.

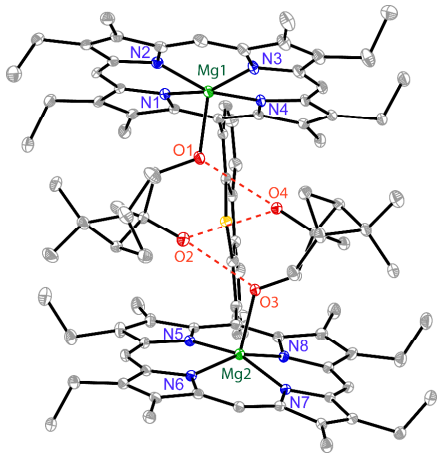

Fig. 2. A perspective view of **1**•$(L^2)_2$ showing 50% thermal contours for all non-hydrogen atoms at 100 K (H atoms have been omitted for clarity).

^{1}H NMR spectra plays an important role in establishing the presence of 1:1 *sandwich* complex in solution. Fig. S10 shows the relevant spectra at 295 K coming from the reaction between **1** and L^1 in $CDCl_3$. Trace A shows the well resolved ^{1}H NMR spectra of **1**, while trace B shows the spectrum after addition of 1.0 M equivalent of L^1 due to the formation of 1:1 *sandwich* complex. Trace C, however, shows the ^{1}H NMR spectrum of free L^1. In the 1:1 *sandwich* complex, the bound –OH peak is upfield shifted to -3.20 ppm. The –CH_3 and –*CH* peaks of L^1 are also upfield shifted by 4.24 and 5.61 ppm, respectively, due to close vicinity with the porphyrin rings. The identical 10 and 20-*meso* protons are now split into two resonances due to chiral environment generated by the interporphyrin stereospecific twisting out of the ditopic binding of the chiral diol. The ^{1}H NMR spectra of crystalline sample of **1**•$(L^2)_2$ in $CDCl_3$ was also recorded (Fig. S11); split in the 10, 20-*meso* protons clearly indicates the presence of chiral environment within the molecule. It has been found that the protons in **1**•$(L^2)_2$ are relatively less upfield shifted compared to the 1:1 *sandwich* complex reported here.

The binding constant between **1** and chiral diols (L) are determined by CD spectroscopic titration method using the HypSpec computer program (Protonic Software, U.K.).[12] Two sets of CD titration data were analyzed considering a binding model with three colored stoichiometric states of Mg(II)bisporphyrin (**1**), 1:1 and 1:2 host-guest complex (Scheme 1). For L^1, K_1 and K_2 are obtained as $3.5 \pm 0.2 \times 10^5$ M^{-1} and 2.4

± 0.3 × 10^3 M^{-1} (Figs. S12 and S13), respectively, while for L^2, the values are 6.3 ± 0.2 × 10^4 M^{-1} and 2.5 ± 0.1 × 10^4 M^{-1} (Figs. S14 and S15). L^3 shows binding constants similar to L^2 (Figs. S16 and S17). Binding constants are also obtained for the complexes using one set of UV-visible spectroscopic titration data (Figs. S18 and S19), however, the values are very similar.

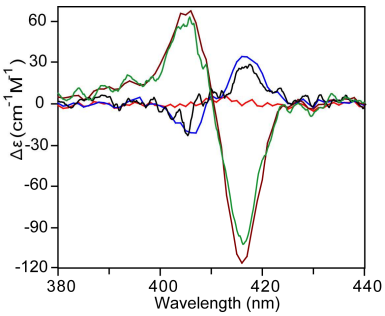

Fig. 3. Calculated CD spectra of **1** (red), **1**•L^1 (blue), **1**•$(L^1)_2$ (brown) and observed CD spectra of **1**•L^1 (black) and **1**•$(L^1)_2$ (green).

The interactions of the chiral diol L with **1** was also monitored in dichloromethane at 295 K using CD spectroscopy. Similar to the observations found in the UV-visible spectra in case of L^1, there appear, in CD spectrum also, two spectral patterns at low and high ligand concentration regions associated with 1:1 *sandwich* and 1:2 host-guest complexes, respectively. Gradual addition of L^1 (upto 50 equivalent) into the dichloromethane solution of **1**, however, generates a low CD signal of amplitude (A_{cal} = 58 $M^{-1}cm^{-1}$) due to the formation of 1:1 *sandwich* complex (Fig. 3). The two porphyrin rings are oriented in a clockwise direction in 1:1 *sandwich* complex in order to have minimum host-guest steric clash. With excess ligand concentration (50 to 843 equivalent), however, the 1:1 *sandwich* complex eventually get converted to 1:2 host-guest complex which displayed an enhanced CD couplet (A_{cal} = -188 $M^{-1}cm^{-1}$) but with opposite sign. As can be seen from the distribution plots (Fig. S13), neither 1:1 nor 1:2 host-guest complex can be exclusively formed at any concentration of L^1 and thus the CD amplitudes have been calculated.

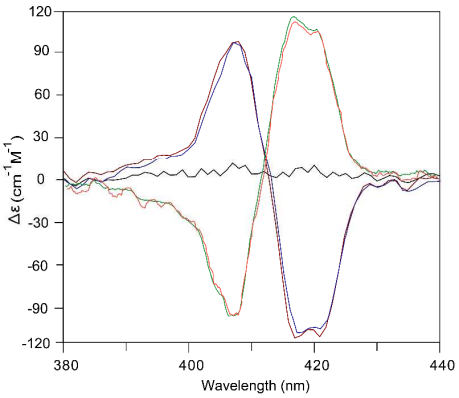

Fig. 4. Calculated CD spectra of **1** (black), **1**•$(L^2)_2$ (brown) and **1**•$(L^3)_2$ (green) and observed CD spectra of **1**•$(L^2)_2$ (blue) and **1**•$(L^3)_2$ (red).

Interaction of the bisporphyrin host **1** with (1*S*, 2*S*, 3*R*, 5*S*)-2,3-pinanediol (L^2) guest in dichloromethane was also monitored by CD spectroscopy and Table S1 summarizes the experimental spectral parameters for all the complexes reported here. Addition of L^2 to the dichloromethane solution of **1** produces exclusively1:2 host-guest complex **1**•$(L^2)_2$ with highly enhanced bisignate CD signal with an amplitude of -215 M^{-1} cm^{-1} (Fig. 4) at the Soret band region which does not change upon further addition of the guest substrate. The remarkably high amplitude bisignate CD signal (A_{cal}, -215 $M^{-1}cm^{-1}$) for **1**•$(L^2)_2$ can be ascribed to the complex's relatively high stability (K_2 = 2.5 ± 0.1 × 10^4 M^{-1}) and formation of a unidirectional left-handed screw twisted around the rigid dibenzothiophene bridge by a torsion angle of -3.80° (*vide supra*). Preorganization of the binding site of the (*R*)-guest ligand has forced two porphyrin macrocycles in **1**•$(L^2)_2$ to be oriented in an anticlockwise direction. CD signal with similar but opposite chirogenic response has also been obtained with other enantiomeric guest (1*R*, 2*R*, 3*S*, 5*R*)-2,3-pinanediol (L^3) (Fig. 4). Presence of tertiary carbon atom immediate to the –OH(2) group generates unbearable steric strains in the 1:1 *sandwich* complex and thus, resulted the formation of 1:2 *endo-endo* complex exclusively. Presence of inter-ligand hydrogen bonding between the –OH groups, as revealed in the crystal structure, stabilizes such an unusual *endo-endo* conformer that also hinder free movement of the guest ligands inside the bisporphyrin cavity. Fig. S20 compares the CD spectral change of **1** in CH_2Cl_2 upon addition of 1 equivalent of L^2, 1 equivalent of L^2 + 1 equivalent of L^3, and 1 equivalent of L^2 + 250 equivalent of L^3. As can be seen, CD sign is controlled solely by the chirality of the substrate; (*S*)-guest shows positive CD couplet while (*R*)-guest produces negative CD couplet which is, in fact, dictated by the projection of the binding site at the chiral center in the 1:2 host-guest complex. CD spectra of **1**•$(L^2)_2$ obtained in solid (using KBr matrix of pure crystals) and in dichloromethane at 295 K have similar spectral features but the solid state spectra is somewhat red shifted compared to the solution phase (Fig. S21). In sharp contrast, enantiopure monoalcohols such as (*S*)-2-butanol, (1*S*)-borneol and (1*S*, 2*R*, 5*S*)-1-menthol bind with **1** to give 1:2 host-guest complexes only but do not generate sufficient chiroptical response (Fig. S22-S24).

1:1 *sandwich* complexes generally incur stronger exciton coupling due to ditopic interaction between the enantiopure chiral guests with bisporphyrin metal centre which results large interporphyrin twist. On the other hand, in the 1:2 complex, guest ligand adopts monotopic interaction with bisporphyrin metal centre and, thus, unable to rope two porphyrin macrocycles much in a preferred direction that lessen or sometimes remove its chirogenic property. In sharp contrast, highly enhanced bisignate CD signals are obtained for **1**•$(L^1)_2$, **1**•$(L^2)_2$ and **1**•$(L^3)_2$ even with a rigid bisporphyrin architecture which are due to unidirectional twisting of the two porphyrin rings in the *endo-endo* conformation that are stabilized by the interligand H-bonding. The absence of H-bonding leads to the stabilization of *exo-endo* conformer resulting negligible chirogenic response as also observed with enantiopure monoalcohols (L^4-L^6).

1:2 host-guest complexes can adopt, in principle, a number of possible conformations namely *endo-endo*, *exo-endo* and *exo-exo*. Geometry optimization of all the three possible conformers for **1**•$(L^2)_2$ are done with the help of DFT in which *endo-endo* conformer (as also observed in the X-ray structure) is stabilized by 3.45 and 8.22 kcal/mol compared to *exo-endo* and *exo-exo* conformer (Fig. S25 and Table S2), respectively, due to the presence of inter ligand H-bonding in the *endo-endo* form.

Anticlockwise twisting of two porphyrin macrocycles in **1**•$(L^2)_2$ has also been obtained in the DFT optimized structure in which a torsion angle (Φ) of -7.62° is observed which is, however, in good agreement with the experiment. It is also interesting to note that even if two macrocycles are twisted manually in the clockwise direction, the optimized structure stabilizes the conformer having anticlockwise twist only. When the unbound –OH of L^2 is replaced by methyl group manually, DFT optimization of 1:2 host-guest complex stabilizes the *exo-endo* conformer by 1.57 and 2.27 kcal/mol compared to *exo-exo* and *endo-endo* conformer, respectively (Fig. S26 and Table S3). Similar trends are also obtained when unbound –OH group of L^2 is replaced manually by –SH group; here also the *exo-endo* conformer is stabilized by 0.5 and 4.14 kcal/mol as compared to *exo-exo* and *endo-endo* conformer, respectively (Fig. S27 and Table S4). All these results support the importance of interligand H-bonding in stabilizing the *endo-endo* form of **1**•$(L)_2$ (L: L^1, L^2 and L^3) which eventually generates large chirogenic response even in 1:2 host-guest complexes.

In summary, the present work demonstrates a clear structural rationalization of the origin of chirality transfer from an optically active guest to an achiral host in a 1:2 host-guest supramolecular complex. Chiral diol binds with the metal centre in an unusual *endo-endo* fashion due to the stabilization out of interligand H-bonding between the -OH groups. Pre-existing chirality of the diol guests has forced two porphyrin macrocycles to be oriented in a stereospecific direction to minimize host–guest steric interactions in which (*S*)-guest shows positive CD couplet while (*R*)-guest produces negative CD couplet in the 1:2 host-guest complex. The highly enhanced bisignate CD signal of 1:2 host-guest complex **1**•$(L)_2$ can be ascribed to the complex's high stability to form *endo-endo* conformation which eventually leads to the formation of unidirectional screw. In sharp contrast, enantiopure monoalcohol with similar structure do not induce chirality to **1** due to lack of inter-ligand H-bonding which is the key element for stabilizing *endo-endo* conformer. A large variety of the ditopic chiral substrates such as amino alcohols, 1,3 diols etc have also been found to behave similarly as in 1,2-diols reported here and further work is in progress.

We thank SERB and CSIR, New Delhi for financial support. CARE scheme of IIT Kanpur is gratefully acknowledged for the CD facility.

Notes and references

[a]*Department of Chemistry, Indian Institute of Technology Kanpur, Kanpur-208016. INDIA. Fax:+91-512-259 7436 ; Tel: +91-512-259 7251; E-mail: sprath@iitk.ac.in*

† Electronic Supplementary Information (ESI) available: synthesis and characterization. UV-visible spectral changes (Fig. S1-S4); Job's plot (Figs. S5, S8), ESI-MS (Figs. S6, S7); Crystal structure packing (Fig. S9), ^{1}H NMR spectra (Figs. S10, S11), CD and UV spectral fitting (Figs. S12-S19), CD titration (Fig. S20), solid state CD (Fig. S21), CD titartion with L^4, L^5 and L^6 (Fig. S22-S24), DFT-optimized structures (Fig. S25-S27), spectral data (Table S1), DFT optimized structural data (Tables S2-S4). X-ray crystallographic details in CIF format.

1 (a) G. Pescitelli, L. D. Bari, N. Berova, *Chem. Soc. Rev.,* 2014, **43**, 5211-5233; (b) E. Schwartz, S. L. Gac, J. L. M. J. Cornelissen, R. J. M. Nolte, A. E. Rowan, *Chem. Soc. Rev*. 2010, **39**, 1576-1599; (c) J. W. Canary, *Chem. Soc. Rev.* 2009, **38**, 747-756; (d) G. A. Hembury, V. V. Borovkov, Y. Inoue, *Chem. Rev.* 2008, **108**, 1-73.

2 (a) V. V. Borovkov, I. Fujii, A. Muranaka, G. A. Hembury, T. Tanaka, A. Ceulemans, N. Kobayashi, Y. Inoue, *Angew. Chem., Int. Ed.* 2004, **43**, 5481-5485; (b) J. M. Lintuluto, V. V. Borovkov, Y. Inoue, *J. Am. Chem. Soc*. 2002, **124**, 13676-13677; (c) V. V. Borovkov, J. M. Lintuluoto, H. Sugeta, M. Fujiki, R. Arakawa, Y. Inoue, *J. Am. Chem. Soc*. 2002, **124**, 2993-3006.

3 (a) S. Brahma, S. A. Ikbal, A. Dhamija, S. P. Rath, *Inorg. Chem.* 2014, **53**, 2381-2395; (b) S. Brahma, S. A. Ikbal, S. P. Rath, *Inorg. Chem.* 2014, **53**, 49-62; (c) S. Brahma, S. A. Ikbal, S. Dey, S. P. Rath, *Chem. Commun.* 2012, **48**, 4070-4072.

4 A. G. Petrovic, G. Vantomme, Y. L. N. Abril, E. Lubian, G. Saielli, I. Menegazzo, R. Cordero, G. Proni, K. Nakanishi, T. Carofiglio, N. Berova, *Chirality* 2011, **23**, 808-819.

5 (a) A. Anyika, H. Gholami, K. D. Ashtekar, R. Acho. B. Borhan, *J. Am. Chem. Soc.* 2014, **136**, 550-553; (b) X. Li, C. E. Burrell, R. J. Staples, B. Borhan, *J. Am. Chem. Soc.* 2012, **134**, 9026-9029; (c) X. Li, M. Tanasova, C. Vasileiou, B. Borhan, *J. Am. Chem. Soc*. 2008, **130**, 1885-1893.

6 (a) I. C. Pintre, S. Pierrefixe, A. Hamilton, V. Valderrey, C. Bo, P. Ballester, *Inorg. Chem.* 2012, **51**, 4620-4635; (b) J. Etxebarria, A. V. Ferran, P. Ballester, *Chem. Commun.* 2008, 5939-5941.

7 (a) H. Kai, S. Nara, K. Kinbara, T. Aida, *J. Am. Chem. Soc***.** 2008, **130**, 6725-6727; (b) T. Muraoka, K. Kinbara, T. Aida, *Nature* 2006, **440**, 512-515.

8 (a) J. Jiang, X. Fang, B. Liu, C. Hu, *Inorg. Chem*. 2014, **53**, 3298-3306; (b) H. Yoon, C. –H. Lee, W. –D. Jang *Chem. Eur. J.* 2012, **18**, 12479-12486.

9 S. Faure, C. Stern, R. Guilard, P. D. Harvey, *J. Am. Chem. Soc*. 2004, **126**, 1253-1261.

10 (a) A. Chaudhary, S. A. Ikbal, S. Brahma, S. P. Rath, *Polyhedron* 2013, **52**, 761-769; (b) S. Brahma, S. A. Ikbal, S. P. Rath, *Inorg. Chim. Acta.* 2011, **372**, 62-70.

11 Crystal data for **1**•$(L^2)_2$, orthorhombic, space group $P2_12_12_1$, a= 13.6073(11) Å, b= 24.816(2) Å, c = 25.860(2) Å, α=90°, β= 90°, γ=90°, V = 8732.5(13) Å^3, Z = 4, Dc = 1.158 Mg/mm^3, T = 100(2) K, No. of reflection used = 16173, θ_{max}=25.499°, R1 = 0.0579 (for I > 2σ(I)), wR2 (all data) = 0.1399, Goodness of fit on F^2=1.047; Largest diff. peak and hole; 0.384 and -0.222 eÅ^{-3}. CCDC-1017376 contains the supplementary crystallographic data for this paper.

12 (a) www.hyperquad.co.uk/ HypSpec.htm. (b) P. Gans, A. Sabatini, A. Vacca, *Talanta* 1996, **43**, 1739-1753.